JTTEE5 1: 117-128

Diagnostics of Thermal Spraying Plasma Jets

P. Fauchais, J.F. Coudert, M. Vardelle, A. Vardelle, and A. Denoirjean

Direct current thermal plasma jets are strongly affected on the one hand by the arc root fluctuations at the anode, resulting in a type of pulsed flow and enhanced turbulence, and on the other hand by the entrainment of surrounding cold gas in the plasma jet. These phenomena and the resulting temperature distributions have been studied using a wide range of diagnostic techniques, including fast cameras, laser doppler anemometry (LDA), coherent anti-Stokes Raman spectroscopy (CARS), Rayleigh scattering, emission spectroscopy, Schlieren photography, enthalpy probes, and sampling probes. The information obtained by these techniques is evaluated and compared. The effect of the arc fluctuations on the spectroscopic measurements is emphasized, and the possibility of using these fluctuations to determine information on the arc behavior and the axial velocity of the jet is presented. Optimization of plasma processing of solid particles requires information about their size and surface temperature, as well as number flux, and velocity distributions at various locations in the flow field. The different statistical techniques of in-flight measurements are discussed together with their limitations. A method to determine the temperature and species density of the vapor cloud or comet traveling with each particle in flight is then presented. However, such statistical measurements present ambiguities in their interpretation, which can be addressed only by additional measurements to determine the velocity, diameter, and surface temperature of a single particle in flight. Moreover, information on single particles is required to understand the coating properties, which depend strongly on the way the particles flatten and solidify upon impact. A method to obtain data related to a single particle in flight and to follow the temperature evolution of the corresponding splat upon cooling is presented. The article concludes with the description of the experimental techniques to follow the temperature evolution of the successive layers and passes. This is important because temperature distribution within the coating and substrate controls the adhesion and cohesion of coatings as well as their residual stress.

1. Introduction

DIRECT current (dc) plasma spraying is a fast-growing technology that has progressively diffused from aeronautic and nuclear industries to other industries. This is due to the increasing need for thick coatings with progressively more sophisticated properties and for better control of coating quality and reproducibility. These results have been possible due to a better understanding of the relevant phenomena resulting from the development of diagnostic techniques, which will be summarized in this article. The thermomechanical properties of coatings, as well as their adhesion and cohesion properties, depend on the following:[1-5]

- Molten state, velocity, size, and density of particles upon impact on the substrate. These parameters are controlled on the one hand by the heat and momentum transfers between the plasma jet and the particles and on the other hand by particle morphology, size, and injection velocity distributions.
- Chemical reactions of the particles with the surrounding atmosphere, especially the entrained air, as well as their possible decomposition or bursting upon penetration into the plasma jet.
- Particle flattening and cooling is linked to the above-mentioned conditions, but as to the nature, roughness, and temperature of the substrate or the previously deposited layers. These parameters control the cohesion and adhesion of the coating, as well as the quenching stresses. Moreover, the heat transfer between the plasma plume, the successive coating layers, and the substrate induces temperature gradients during spraying, which vary during cooling. These variations control the residual stresses and cracking within the coating.

Key Words: experimental techniques, particle temperature, particle velocity, plasma diagnostics, review article

P. Fauchais, J.F. Coudert, M. Vardelle, A. Vardelle, and **A. Denoir-Jean,** Laboratoire de Céramiques Nouvelles, University of Limoges, France.

The heat and momentum transfer between the plasma jet and the particles depend, among other parameters, on the temperature and velocity distributions of the plasma jet. Therefore, modeling and prediction of these quantities is mandatory. However, many problems are still pending for such measurements. In general, this is due to the continuous fluctuations of the plasma jet,[6] with a pulsed flow that is related to the surrounding gas entrainment mechanism. It is an engulfment type of process[7] that plays an important role with regard to chemical reactions in flight and during cooling of the plasma jet. The temperatures needed for the calculations are the electron (T_e) and heavy species (T_h) temperatures, which are not directly accessible. For velocity, no method seems to yield reliable results[8,9] at the present time. To calibrate the models, it is also necessary to measure the velocity, number density, diameter, and surface temperature of the particles in flight. However, for dc plasma jets, only distributions are measured, and the interpretation of the results, especially for surface temperature, is not straightforward.[10,11]

A basic understanding of plasma coating formation requires knowledge of the thermal history of the droplets during their flattening and cooling process. These mechanisms have received much less attention than those related to particles in flight.[12] Although many micrographs of single particles collected during spraying have been published, their interpretation is still questionable due to the lack of information about the velocity, diameter, and surface temperature of the particles upon

impact, as well as the cooling rates of the splats. The first known measurements of droplets cooling during and after flattening have been available only recently. The cooling of the splats from more than 3500 K to less than 2000 K takes place in a few tens of microseconds and seems to depend not only on the substrate or the nature of the previously deposited layers, but also on their temperature. The material deposited in a single pass of the torch (resulting in a single bead with a roughly Gaussian shape, see Section 4) cools in times on the order of milliseconds at temperatures below 2000 K, depending on factors such as the powder feed rate and the velocity of the torch relative to the substrate. The cooling rate is also affected by the relative torch-to-substrate motion, the time and amount of overlap between successive beads (resulting in passes), and the use of auxiliary cooling devices. Temperature gradients within the substrate and the cooling cause residual stresses within the coating and substrate that can induce cracking, especially in ceramic deposits.

2. Plasma Jet Measurements

2.1 *General Remarks*

Before describing the experimental measurements, it is important to recall briefly how the plasma jet is generated. The plasma column expansion from a tiny molten spot (a few tenths of a square millimeter) at the cathode tip is strongly affected by the cold plasma gas flow close to the cathode tip, as well as the nature and the flow rate of the gas and the arc current.[13-16] This flow depends on the cathode cone angle and diameter and on the arc chamber and gas injector designs, as well as the nozzle diameter and design.

When the cold boundary layer close to the anode-nozzle wall is hot enough (and this is correlated to the plasma column expansion), then the arc strikes at the anode wall by one or a few tiny plasma columns that are continuously fluctuating under the action of the drag force and the $j \times B$ (*i.e.*, current × magnetic flux) forces.[13] These fluctuations continuously modify the length of the electrically conducting plasma column. Thus, the voltage presents a saw-tooth shape, with frequencies varying between one and a few tens of kiloHertz.[15,17] These fluctuations in the plasma column length (linked to the gas aerodynamics in the nozzle), coupled to the negative resistance of the arc, react with the power supply, which brings in its own fluctuations (generally, at frequencies below 600 Hz). All these phenomena induce pulsating plasma jets.[18] These pulsations, together with the large velocity difference between the plasma jet and the surrounding atmosphere, cause large-scale eddies and the onset of turbulent flow.[7]

To summarize, the plasma jets to be analyzed (1) are continuously fluctuating (equivalent to a type of pulsing flow), with a certain correlation between electric and aerodynamic fluctuations; (2) highly turbulent in their fringes and in their plume, with nonisotropic velocity fluctuations;[17] (3) present high radial temperature gradients (up to 4000 K/mm);[8] and (4) have an engulfment-type entrainment mechanism,[19] with cold surrounding gas "bubbles" (higher density and thus inertia than their high-temperature surroundings) entrained in the hot plasma jet. These bubbles do not mix with the plasma, at least initially.

2.2 *Arc Fluctuations and Turbulences*

2.2.1 *Video Cameras*

Computerized video-image processing and process-control software make it possible to automatically extract information from video images. For example, in Control Vision's laser-enhanced stroboscopic video system,[20] an electronic image of the process is captured using momentarily intense light from a strobe illumination unit rather than using the light from the process itself. The system provides real-time pictorial information on the dynamic behavior of the plasma jet or of particles (in the solid or molten state) moving at high speeds within the most intense plasma jets.[18]

For plasma jet fluctuations, it is also possible to use video cameras with shutter speeds up to 10^{-4} to 10^{-5} sec. Such measurements (performed with strobe illumination,[21] or with a simple video camera) have shown that the plasma jet, which with the naked eye looks stable and axisymmetric, is in fact continuously fluctuating in length (up to 50 to 60%) and in position. The extremity of the bright core moves radially and axially in a random manner. For a given nozzle diameter, these fluctuations seem to depend on the flow close to the cathode tip, the gas nature and flow rate, and the arc current. However, to obtain more precise information (such cameras have a time resolution of 10 to 60 frames), other measurements are necessary.

2.2.2 *Spectral Analysis*

Spectral analysis is a nonintrusive diagnostic technique capable of providing a great amount of information about the operating conditions of a plasma torch.[17] Analysis of pressure fluctuation, for example, through acoustical spectral measurements with an omnidirectional microphone provides information about the flow structure due to the arc root motion, especially in the fringes of the plasma column. Furthermore, by spectrally analyzing the signals from a photomultiplier or a photodiode focused on the axis of the plasma jet at a given location, one can gain insight into the temperature fluctuations of the jet and how they correlate with the arc root motion. The voltage fluctuations are due to the axial motion of the arc column and/or of the anode arc root. Coupling with the power source response can be deduced from the simultaneous study of arc current fluctuations. The first measurements presented by Pfender *et al.*[17] indicate that the relationship between internal and external perturbations is rather weak. The main parameters influencing the fluctuations seem to be the same as those already underlined for the video camera measurements, with a more pronounced effect of the flow rate. However, an appropriate signal treatment with adapted filters[22] before cross correlation produces better correlations. These measurements could also probably give information about electrode erosion, but considerable additional work is needed to better understand the phenomena involved.

2.2.3 *Shadowgraphy*

Shadowgraphs of plasma jets[23,24] reveal the abrupt development of turbulence from a well-behaved laminar flow near the nozzle exit. They reveal typical shear layer instabilities close to the nozzle exit, characterized by the formation of vortex rings

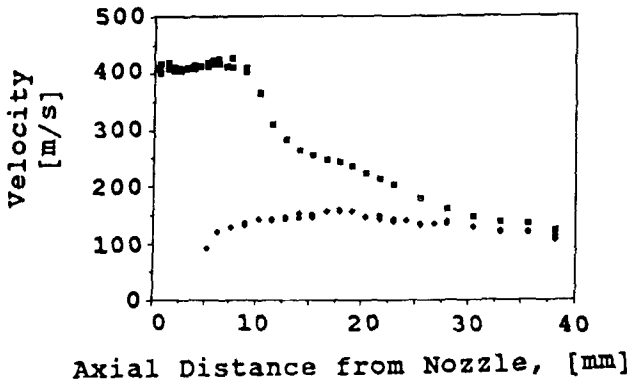

Figure 1 Comparison of plasma jet and entrained fluid velocity on jet center line (argon plasma, 23.6 slm, 450 A, 24 V). After Pfender *et al.*[24]

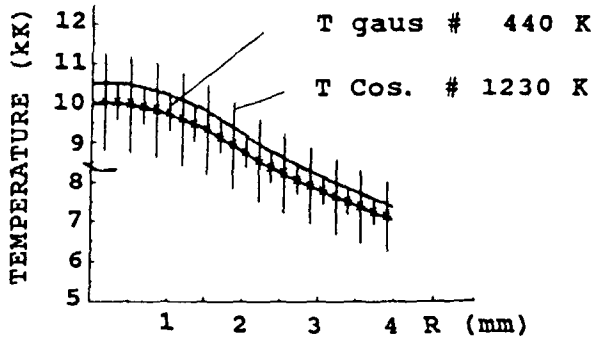

Figure 2 Comparison of the radial temperature distribution deduced from the time-averaged intensity (–) and the stationary component of the temperature obtained after signal treatment (static rectifier, P = 23.2 kW, 290 A, 50 slm N_2, anode 7-mm inside diameter). After Ref 28.

around the plasma jet. Farther downstream, the vortex structure breaks down over a relatively short distance, resulting in large-scale turbulence eddies that rapidly penetrate into the core of the plasma jet. The location of the transition zone[24] is thought to be driven by the rapid cooling of the jet and the resulting increase of the Reynolds number, from about two orders of magnitude at the torch exit to four orders of magnitude in the transition zone. Here also, the arc current and the gas flow rate play an important role.[24] However, the respective influences of the pulsations of the plasma jet and of the large velocity difference between the plasma jet and the surrounding atmosphere in the development of the turbulences are not yet understood.

2.2.4 *Turbulence Measurements*

Turbulence intensity measurements have been performed[17,24] by using laser doppler anemometry of small alumina particles ($d < 3$ mm). They were injected from a specially designed fluidized bed,[25] inside the nozzle and downstream of the arc root. The turbulence was defined as the ratio of the standard deviation of the individual velocity measurements for a given data point divided by the maximum center line mean velocity for a given axial distance downstream. As for the shadowgraphs, the results show the rapid increase of the axial velocity fluctuations at the jet edge due to the mixing and entrainment of external air.

By injecting the small alumina particles around the plasma jet, the velocity of the entrained air was measured along the center line of the plasma.[24] Such measurements, illustrated in Fig. 1, show that with the given conditions, for $z \leq 30$ mm, the fluid from the plasma jet has a much higher mean velocity than the entrained gas that has reached the center line at a distance of about 8 to 10 mm. Entrained air does not mix well with the plasma gas initially, but instead travels with a much slower mean velocity than the plasma, thus forcing the plasma gas to flow around it. Such measurements are confirmed by coherent anti-Stokes Raman spectroscopy (CARS) (see Section 2.3.3). This seems to indicate that the more classical belief of entrainment and mixing by stochastic small-scale eddies is not a realistic picture of the transport mechanisms in turbulent plasma jets.

2.3 *Temperature, Velocity, and Concentration Measurements*

2.3.1 *Instant or Mean Values*

The techniques used are mainly emission spectroscopy, laser scattering, and enthalpy probes. Enthalpy probes give Favre averaged values and cannot follow the plasma jet fluctuations and/or turbulence. Local measurements (according to the size of the probe) can be performed.

The measurement, by laser anemometry, of the velocity of small particles injected in the plasma jet can give the time-averaged flow velocity, provided they have traveled a minimum distance in the jet before the measurement point to overcome the Knudsen effect.[17,24] Such measurements also allow determination of the velocity dispersion due to the different treatments undergone by the particles according to the dimensions of the measurement volume and the size of the particles, which is not necessarily small compared to the turbulence eddies. For example, Spores[26] indicates that up to 10% of the measured dispersion, often called turbulence, is associated with the size distribution of the seed particles.

For CARS experiments, the entire CARS spectrum can be generated simultaneously on the time scale of the laser pulse.[23] It is thus an instant measurement with a high spatial resolution when using crossed beam geometry.

Rayleigh scattering measurements are performed using either a pulsed Yag laser with boxcar averaging[27] or CW lasers with lock-in amplifier detection. Thus, time-averaged results are obtained. Here also, a high spatial resolution can be achieved.

Emission spectroscopy can be performed using either photomultipliers with a very fast response time (10 nsec can be achieved and large fluctuations correlated to those of the plasma jet can be observed for the intensity signals), or with an optical multichannel analyzer (OMA) giving time-averaged signals. Such measurements are, of course, along the line of sight,[8] and Abel's inversion has to be performed to obtain local measurements.

As the relationship between the line intensity and temperature is not at all linear, a time-averaged intensity does not permit direct determination of temperature from time-averaged meas-

urements. The signal has to be processed to extract the stationary component of temperature,[28] which may be quite different from the temperature deduced from the time-averaged signal, as illustrated in Fig. 2. In this figure, the error bars marked "gaus" correspond to the temperature fluctuations due to the random attachment of the arc root in the nozzle (described by a Gaussian noise), whereas the larger error bars (T_{cos}) correspond to the power source fluctuations.

2.3.2 *Temperature Measurements*

2.3.2.1 *Emission Spectroscopy*

Such measurements give the population of the emitting level, and assumptions must be made to determine a temperature from this population.[8] Thus, depending on the assumptions, different temperatures can be measured.

The rotational temperature, from 4000 to 11,000 K (in general from N_2^+ spectra), can be measured with either a few percent of nitrogen introduced in the plasma jet or using that of the entrained air. This temperature can generally be assumed to be that of the heavy species, T_h, due to the very short relaxation time between translation and rotation ($\sim 10^{-8}$ sec).[8]

The excitation or population temperatures are determined from atomic lines, with values between those of heavy species and electrons ($7000 < T < 15{,}000$ K). Temperatures can also be deduced from the continuum nearer to T_e than to T_h ($8000 < T < 15{,}000$ K).

In Fig. 3, the error bars for T_{rot} correspond to:

$$\delta T = \sqrt{2E_m / \frac{\partial^2 Eq}{\partial T^2}}$$

where E_m is the minimum of a quantity that allows determination of T_{rot}[16] and is related to the signal to noise ratio, whereas $\partial^2 Eq/\partial T^2$ is related to the sensitivity of the method.

These different temperatures are not necessarily in equilibrium among themselves. This is illustrated in Fig. 3 for a dc nitrogen plasma jet flowing in a controlled-atmosphere chamber filled with nitrogen at a pressure of 33 kPa.[16] Of course, in such pressure conditions, the nonequilibrium effects are somewhat enhanced, but the trends are the same as those at atmospheric pressure. The temperatures deduced from atomic excited states (T_{poph}, T_{popb}), from continuum (T_{cont}), and from the band head (T_{band}) are higher than those obtained from the rotational spectra, especially in the fringes of the jet where the diffusion of the electrons is important.[29]

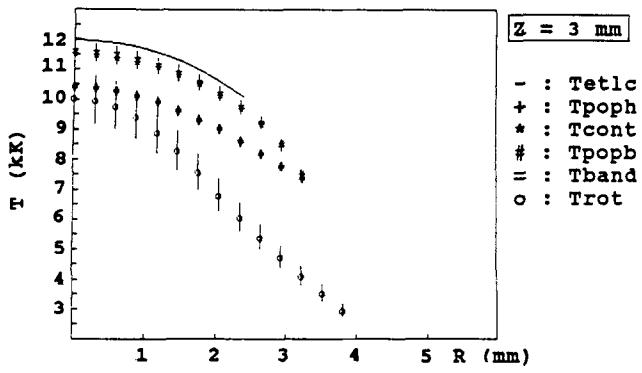

Figure 3 Temperature distributions measured 3 mm downstream of the nozzle exit of a dc plasma jet (cylindrical nozzle 6 mm in diameter, 250 A, 82 V, thermal efficiency 71%, 40 slm N_2, p_{ch} = 33 Pa). T_{poph} NI 532.8 nm; T_{popb} NI 746.8 nm; T_{band}: band head of N_2^+ 1^-, 0-0; T_{rot}: rotational spectra of N_2^+ 1^-, 0-0; T_{cont}: $\lambda = 531$ nm.

Similar results were obtained with argon plasmas.[30] This clearly indicates that measurements performed with atomic lines have to be considered as trend indicators that provide only relative information, for example, to compare torches or working conditions.

For example, Fig. 4 illustrates the cooling of an argon-hydrogen plasma jet at atmospheric pressure when flowing successively in argon (ionization at 15,000 K), nitrogen (dissociation at 7000 K), and air (oxygen dissociation at 3500 K). It can be seen also with these time-averaged measurements that the jets are rather symmetrical, as when viewed with the naked eye.

Such measurements[31] also confirm the influence of the plasma gas injector design on the turbulent mixing with the surrounding air, as illustrated in Fig. 5. It can be seen that, when injecting the plasma gas radially close to the cathode tip, the length of the plasma jet is drastically reduced compared to that obtained when injecting the gas along the cathode. In both cases, the voltages are the same within 2%, and the thermal efficiencies differ by less than 3%. These time-averaged measurements demonstrate the strong coupling of the turbulent mixing with the "pulsed flow."

2.3.2.2 *Laser Scattering*

Coherent anti-Stokes Raman spectroscopy (CARS) has the advantage of high conversion efficiency, a laser-like coherent signal beam for high collection efficiency, excellent fluorescence and luminosity discrimination, as well as high spatial and temporal resolution.[32,34] It has been used for plasma spray jets,[23] and a broad band approach has been used to generate the entire CARS spectrum on the time scale of the laser pulse. Temperatures were derived from the spectral distribution of the

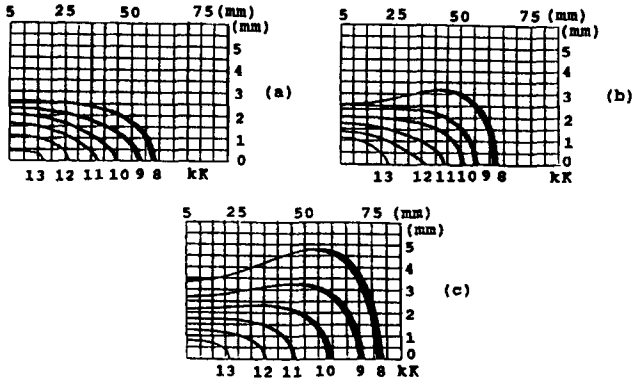

Figure 4 Temperature distributions for an argon-hydrogen plasma jet at atmospheric pressure (P = 34 kW, 81 slm Ar, 9 slm H_2) flowing in air (**a**), nitrogen (**b**), and argon (**c**).[31]

CARS signal using a quick-fit technique based on the full-width at half maximum of the spectral signal. The temperature determination was calibrated against a Pt, Pt-Rd thermocouple. The nitrogen molecular spectra have been used to determine the temperature of surrounding air pumped by an argon plasma jet,[24] as shown in Fig. 6.

Integrated Rayleigh scattering measurements have been performed in the fringes of argon dc arcs or jets flowing in argon, using either chopped CW lasers[35,36] or pulsed Nd:YAG lasers.[27] The light scattered through an angle of 90° was focused onto the entrance slit of a monochromator and detected using a photomultiplier. Such measurements give the density of the neutral species, provided the scattering cross sections are known. At atmospheric pressure, the density of such particles becomes very low for temperatures higher than 8000 K, which is about the limit of the method. Such measurements, which have to be calibrated with gases of known temperatures, also show a strong discrepancy in the jet fringes when comparing the temperatures measured by emission spectroscopy from atomic lines and those deduced from Rayleigh scattering (see for example Ref 27). Problems related to measurements in gas mixtures, such as argon-hydrogen-air (air pumped in the plasma plume), must also be addressed.

2.3.2.3 *Enthalpy Probes*

New computer-controlled systems of small size ($d < 3$ mm), inducing low perturbations of the flow, are available[17,24] to determine temperatures between 11,000 and 2000 K in argon plasma jets and somewhat lower temperatures in argon-hydrogen jets (maximum heat fluxes of 10^6 W/m^2). Figure 7[24] shows some typical results obtained in an argon dc plasma jet and compared to population temperatures determined by emission spectroscopy. The comparison of the two methods shows substantial deviations of the temperatures, especially in the jet fringes. With the fast diffusion of electrons in the cold regions, the population of the excited atomic states, due to inelastic collisions with electrons, is enhanced, and the temperature deduced from this population is overestimated. Moreover, spectrometric measurements refer only to the high-temperature plasma and not to the cold gas entrained into the plasma plume, whereas enthalpy probes measure average temperatures resulting from both hot and cold gases.

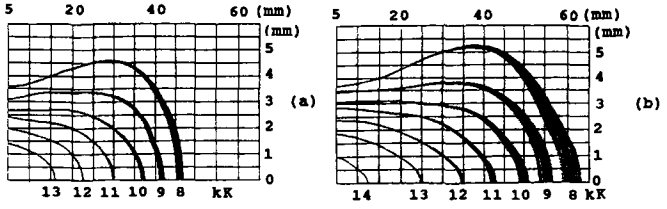

Figure 5 Temperature distributions for argon-hydrogen plasma jets obtained with the same plasma torch (cylindrical nozzle): d = 7 mm, 500 A, 30 slm Ar, 21 slm H_2) with two different gas injectors. (**a**) Radial injection and (**b**) injection along the cathode.

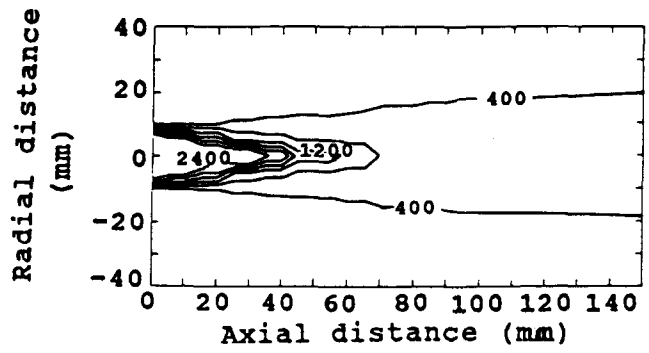

Figure 6 Contour plots of nitrogen temperature for an argon plasma jet in air (250 A, 9.8 slm Ar, 10 kW) after Fincke *et al.*[23,24]

2.3.3 *Concentration Measurements*

Coherent anti-Stokes Raman spectroscopy has been used in dc argon plasma jets to probe the average concentration of nitrogen, from the surrounding air, entrained in the plasma jet.[24,37] Concentration was derived from the strength of the CARS signal. The measurement was calibrated by varying the concentration of premixed air in a cold argon jet. Figure 8 shows the resulting contour plots of nitrogen concentration for a 10-kW argon

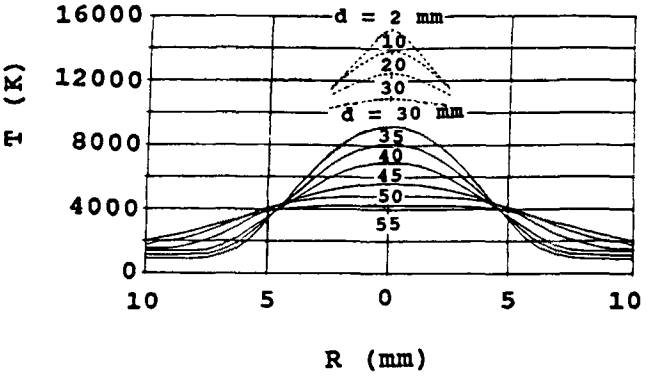

Figure 7 Temperature profiles of an argon plasma jet in argon atmosphere (400 A, 100 scfh Ar, 47 scfh He, $p = 10^5$ Pa, d = distance from nozzle).[24] Atomic emission spectroscopy (.....). Enthalpy Probes (—).

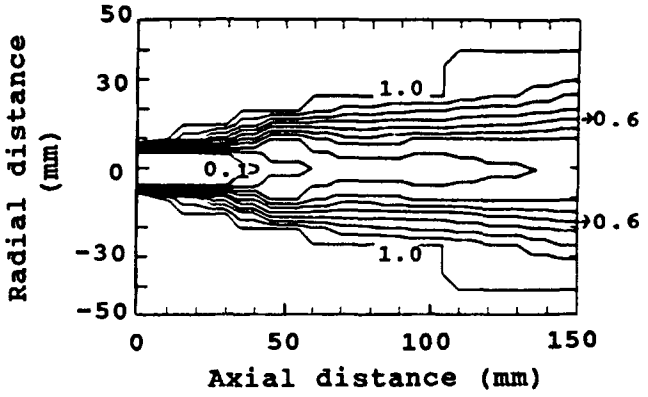

Figure 8 Contour plots of nitrogen concentration for a 10-kW argon torch power (anode, 9.52-mm inside diameter).

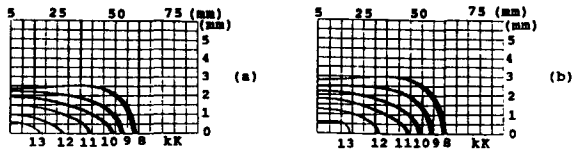

Figure 9 Temperature distributions for argon-hydrogen plasma jets (75.6 slm Ar, 14.4 slm H_2, nozzle diameter 6 mm). **(a)** 35 kW and **(b)** 50 kW.

torch power. The rapid entrainment of air into the core flow of the jet, coincident with the onset of turbulence and jet break-up, is evident in the concentration contours. Such a transition region is not as evident in the associated temperature field (see Fig. 6).

Experimentally, argon concentrations were derived from samples taken with an enthalpy probe.[17,38] The results, which were only available from $z = 20$ mm and farther downstream, show a large drop in center line concentration between the 25- and 35-mm profiles, indicating the end of the potential core. In good agreement with the CARS and LDA measurements (see Sections 2.3.2.2 and 2.3.4), more than 50% air was observed for distances greater than 30 mm. The air pumping increases with the gas flow rate. When the arc current increases, the air pumping occurs at longer distances due to the higher viscosity of the plasma jet. However, as shown by spectroscopic measurements, when the arc column diameter becomes close to that of the nozzle, the length of the jet tends to a limit. This is illustrated in Fig. 9, in which it can be seen that the radius increases from 35 to 50 kW, whereas the length remains almost constant.

2.3.4 *Velocity Measurements*

Flow-velocity measurements are not as well established as temperature-measurement methods. Laser velocimetry[8,39-41] has been used to measure solid particle velocities in a thermal plasma environment. In most gases, it is generally assumed that the velocity of the fine particles (<5 mm) equals the gas velocity, but this may not be the case in plasma flows where the Knudsen effect is enhanced.[42] For example, when injecting the particles inside the nozzle of a dc argon plasma torch downstream of the arc root, the maximum velocity of the particles was reached only 15 mm downstream of the nozzle exit.[43]

The velocity of argon plasma jets has also been determined by observing the doppler shift of fluorescence lines,[44,45] but the obtained values seem to be overestimated. Pitot probes have been successfully used to determine a Favre averaged velocity at distances from the nozzle exit greater than 30 mm for argon dc plasma jets.[46]

Measurements based on either natural or imposed[47] fluctuations of the jet have been developed. In the laboratory, the random attachment of the arc root in the nozzle has been used. It induces variations of the volumetric energy density in the plasma, and these homogeneous regions are entrained by the flow. The light intensity fluctuations sampled at two different points along the jet axis are correlated after a proper signal treatment—for example, elimination of the noise from the first signal followed by a filtering of the second signal with a filter calculated from the filtered first signal. In this case, a sharp cross-correlation function between the two filtered signals could be determined, permitting a measurement, with reasonable accuracy, of the time shift between the two signals and thus the axial velocity of the flow.

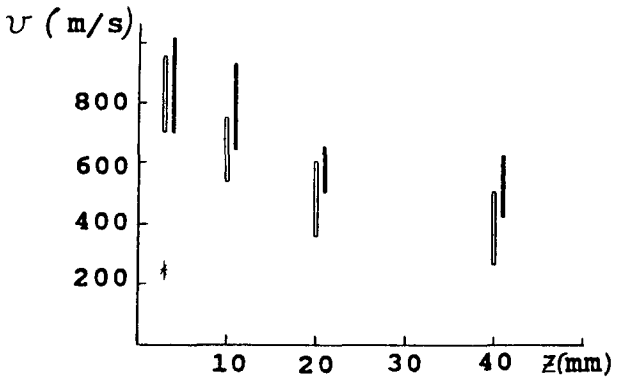

Figure 10 Evolution along the plasma jet axis of the velocity of the flow for three hydrogen percentages (nozzle: 7-mm inside diameter, 200 A, 22 slm Ar^+, +3, +5 slm H_2).

Figure 10 illustrates results obtained for argon-hydrogen plasma jets. The error bar represents the standard deviation for 50 measurements. The increase of the hydrogen percentage gives more impulse to the jet, with the result that the velocity decreases more slowly. The difference in velocity with pure argon is almost a factor of 3, in good agreement with the ratio of the power levels (also about 3) for the same arc current.

3. In-Flight Particle Measurements

Measurement problems are complex. The high temperatures (9000 to 15,000 K in the plasma jet core) result in very intense plasma emission, which makes it difficult to detect scattered light or light emitted by hot particles.[8] This results in a size limitation to detect the light scattered by particles in the plasma core. This limitation depends on the power of the CW laser that is used to illuminate the particles. For example, in typical plasma spray jets (argon-hydrogen 25 vol.%, 40 kW) a 1.5-W argon ion laser line allows one to follow particles down to 1 μm in diameter. For particle surface temperature, the plasma emission makes any measurement in the plasma core impossible.

The high velocities (up to 400 m/sec) and the resulting very short residence times of particles in the small measurement volumes (a few thousands of cubic microns) make it difficult to track the steep gradients.[8] The particles have wide trajectory distributions, resulting from their size and injection velocity distributions.[48] Thus, particles having different sizes, velocities, and surface temperatures travel in the same measurement volume.

3.1 *Qualitative or Semiqualitative Measurements*

The oldest techniques are those using a cine-streak photography technique. For example, see the work of Lewis and Gauvin in 1973[49] in an atmospheric dc jet, or more recently, the work of Frind *et al.*[50] to determine statistical values of the velocities

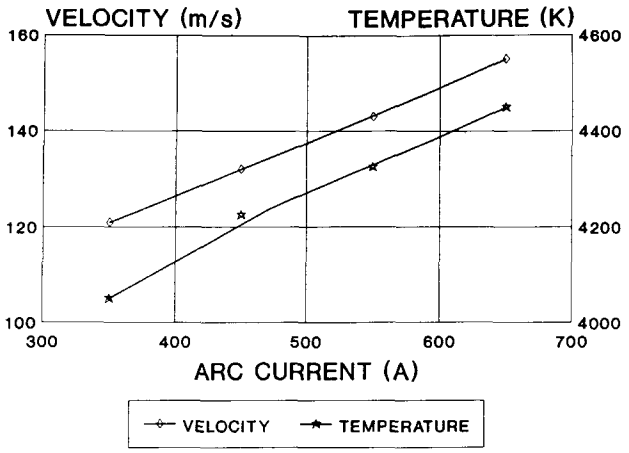

Figure 11 Evolution with the arc current of the velocity and surface temperature of carbide particles injected in an argon-hydrogen plasma jet (72 slm Ar, 18 slm H_2). The measurements were taken 100 mm downstream of the nozzle exit along the mean particle trajectory.

of particles in a low-pressure (5.5 10^3 Pa) dc plasma jet under supersonic flow conditions.

Recently, two-dimensional laser imaging has been presented, which provides information on the particle distributions within the plasma jet according to the power level, gas flow rate, powder injector location and i.d. carrier gas flow rate, etc. A planar laser sheet (obtained with a cylindrical lens and a frequency doubled Nd-YAG laser) about 300 mm in thickness is positioned at different distances from the plane defined by the plasma jet and the powder injector.[51] The 90° scattered light is recorded via a computer-controlled two-dimensional array detector and stored in a digital frame storage unit. The background light from the plasma is considerably reduced by using a narrow band pass filter (3 nm) centered at the laser wavelength and appropriate gating (100 nsec).

3.2 *Quantitative Measurements*

3.2.1 *Velocity, Size, and Surface Temperature*

In fact, the information that is needed is the velocity, surface temperature, and diameter of a single particle at a given position. Such measurements, based on the light pulse method, have been developed by Sakuta and Boulos[52] in RF plasmas, where particle velocities are below 50 m/sec. Their system has never been tested for dc plasma jets, but with fast response times (~1 nsec), it could probably work. A system based on the use of two double wavelength optical fiber pyrometers developed by Vardelle *et al.*[53-55] allows one to determine the velocity and surface temperature of a single particle in flight in dc plasma jets or during its flattening.

Nevertheless, all of the particle measurements performed in dc plasma spray jets are statistical measurements.[8,19,57-61] The velocity is measured by laser velocimetry either using doppler or two focus methods. The flux number density is determined by counting the number of signals obtained from the particles crossing the velocity measurement volume. The particle diameter measurement is based on Mie theory, correlating for example the laser doppler signal pedestal amplitude to the diameter of the particle, which is assumed to be spherical.[62] However, the trajectory ambiguity (particles passing through the center of the edges of the measurement volume of the laser doppler anemometry) has to be removed.[61] Because of this ambiguity, simultaneous measurements of the size and velocity distributions are achieved, but not simultaneous measurements of the size and velocity of single particles. Of course, in all the cases, the measurement volume can be moved across the plasma jet to obtain radial distributions either in one direction or in two orthogonal ones. For example, in the last case, this allows one to determine a two-dimensional particle distribution in a cross section of the plasma jet at a given stand-off distance. The thermal history of the particles is monitored by two-color pyrometry. However, the interpretation of the results must be made cautiously for two reasons. Firstly, the measurement volumes for velocity, number density, and size are not necessarily the same as volumes measured for the surface temperature. Also, the counting can also be quite different for the various measurements. If practically all the particles passing through the measurement volume are taken into account for flux measurements, then some signals for laser velocimetry or size can be rejected, and the corresponding mean values are calculated for a different number of particles than that used for the flux. For temperatures below 2000 K, no signal is detected, and thus only the hot particles are observed, even if the velocity and/or size of the cold particles are measured. It is, however, possible to take into account only the size of the particles giving a temperature signal.[61] In spite of all these drawbacks, such measurements are very useful. For example, Fig. 11 illustrates the influence of the arc current on the axial velocity and temperature profiles for carbide particles in an argon-hydrogen plasma 100 mm downstream of the nozzle exit along the mean trajectory. It can be seen that the velocity increases by 40 m/sec (35%) when the arc current is raised from 350 to 650 A, and the temperature increases by 400 K, *i.e.*, only 10%, and is in good agreement with the decrease in the residence time.

Such a low increase in temperature when the gas enthalpy is raised by almost 90% is due to the fact that the length of the plasma jet increases very little (see Fig. 9), whereas its velocity is almost doubled, thus reducing the residence time of the particles. Notice, however, that in the special case of these heavy carbide particles the increase in their velocity is only 27% against 100% for the plasma.

In Fig. 12, the constriction of the plasma jet when the gas flow rate is increased can be seen. In spite of a higher velocity with a higher flow rate, the surface temperature of the particles is increased. The result is very clear here because a long nozzle with gradually increasing diameter was used to reduce pumping of the surrounding air. Without this extended nozzle and with an external powder injection, the increased gas flow rate induces more air pumping, thus cooling the plasma jet even more rapidly, and surface temperatures are almost the same for both flow rates.

3.2.3 *Vaporization*

Although the importance of particle vaporization under thermal plasma conditions has been stressed in a number of theoreti-

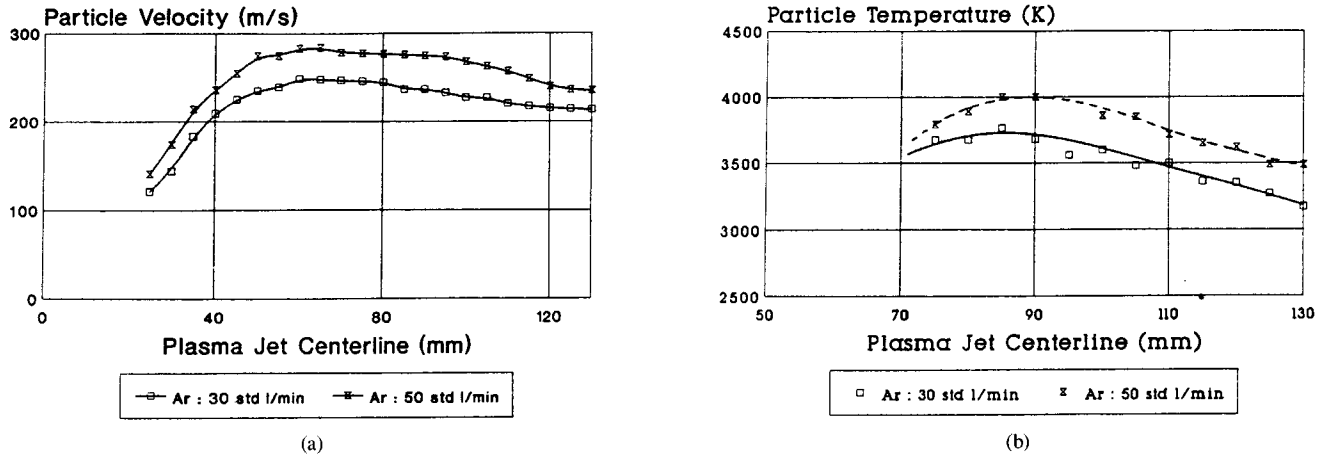

Figure 12 Evolution along the plasma jet axis of the velocity (**a**) and surface temperature (**b**) of yttria particles injected in the diverging region of a long PTF4 plasma torch (nozzle: 7-mm inside diameter, 440 A) for two different plasma gas flow rates—30 slm Ar, 12 slm H_2 (**a**) and 50 slm Ar, 12 slm H_2 (**b**).

cal analyses (see Ref 12), very few experimental data are available concerning this phenomenon. When vaporization occurs, mass transfer from the particle surface toward the plasma gas reduces the effective heat transfer. The vapor diffusion modifies the plasma gas composition and its transport properties. Finally, the vapor cloud may modify the flattening behavior of the droplet.

The presence of metallic vapors in the plasma jet can be evaluated by adsorption spectroscopy. This allows one to determine the ground and metastable state populations of metal atoms or ions resulting from the decomposed vapor[63] (for example, cobalt from cobalt particles or aluminum from AlO emitted by Al_2O_3 particles). Measurements are carried out along the mean trajectory of the particles using a hollow cathode lamp as the light source. For example, such measurements have shown that when alumina particles were sprayed at 15 kW with pure argon as the plasma forming gas, it was possible to measure the aluminum concentration ($n_{Al} \sim 10^{16}$ m^{-3}) 20 mm downstream of the nozzle exit. For an argon-hydrogen mixture (20 vol.%) with P = 17 kW, due to the much better heat transfer, the aluminum atoms were detected 7 mm downstream from the nozzle exit with a maximum concentration (~3.10^{19} m^{-3}) at 30 mm downstream. For greater distances, due to the cooling of the plasma, n_{Al} decreased progressively with densities on the order of 10^{17} m^3 at 100 mm downstream of the nozzle exit.

Detering and Eddy[18,64] have studied by emission spectroscopy and computerized video-image processing argon-helium plasma jets either free of particles or loaded with NiAl or WC-Co powders. The spectroscopic measurements show that the particles (especially W and Co for the cermet particles) are significantly vaporized and ionized, resulting in argon-helium-metal vapor plasmas that deviate significantly from local thermodynamic equilibrium (LTE) with the presence of metal vapors. The nanosecond video frames of the loaded plasma jets show the powder plasma comets, generated during the process, traveling with their particles.

Vardelle *et al.*[63] have developed a technique based on emission spectroscopy to study these vapor clouds surrounding each particle. The temperature in the "diffusion zone" surrounding one particle is determined by the intensity ratio of the vapor lines measured simultaneously. The vapor radius is deduced from the measurement of the vapor concentration around the particle in flight together with the particle velocity (by laser anemometry). The vapor concentration is calculated from the absolute line intensity profile, once temperature is known. Besides the assumptions made under equilibrium conditions in the vapor cloud, such measurements imply symmetrical vapor clouds and can be performed only in regions where the plasma velocity is close to that of the particles. The results, at a given location, correspond generally to an average calculated on 20 events. For example, Fig. 13 shows the cobalt concentration distributions for WC-Co particles in an argon-hydrogen plasma jet. The radius of the clouds is estimated to be on the order of 1 to 1.5 mm (one order of magnitude higher than the particle diameter) and corresponds to 10% of the maximum value of the concentration profiles. The temperature is nearly constant within the vapor cloud and is about that of the plasma jet at the same distance from the nozzle exit. The cobalt concentration is fairly high (~10^{23} m^{-3}) near the particle wall. The evolution of the comet radii at different radial locations may be explained by the different trajectories followed by the various particles investigated.

4. Particle-Substrate Interactions during Spraying

A droplet flattens either on the substrate or on already solidified droplets and experiences radial spreading of the liquid and solidification in times on the order of a few tens of milliseconds.[65,66] According to the powder mass flow rate and the torch-to-substrate relative velocities, the flattened and solidified droplets form in times of the order of milliseconds as a thick sprayed bead, with a shape that is roughly Gaussian. Then the

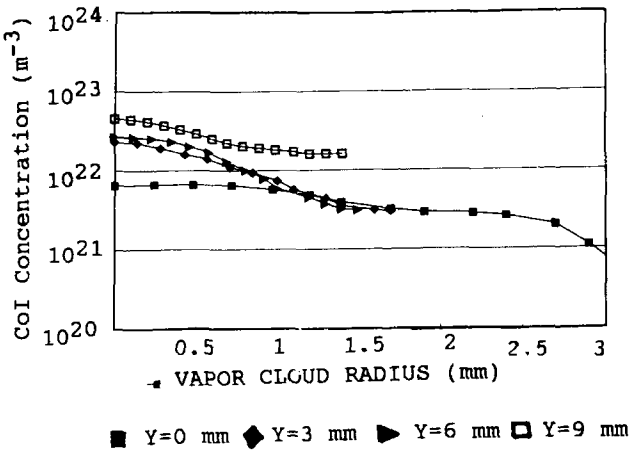

Figure 13 Cobalt concentration distribution within the comets (60 mm from the nozzle exit, 7-mm inside diameter nozzle) for different distances *Y* from the plasma jet center line (600 A, 45 slm Ar, 15 slm H_2, WC-Co particles: –44 +10 μm).

beads overlap to form passes, the coating being made of a given number of successive passes. The beads and passes are heated by the plasma jet plume and the impacting particles and cooled, if necessary, by air or liquid gas jets. Cooling is of primary importance because the temperature gradients within the coating and the substrate, together with the quenching stresses within the individual lamellae, control the residual stresses and the resulting macrocracks.

4.1 *Study of Individual Droplet Flattening*

Many studies have been devoted to the study of the shape of flattened droplets or splats collected on translated or rotated substrates (usually glass slides) crossing the flow.[12] The collected splats exhibit various morphologies, from completely circular discs to exploded particles. The simplified models,[65-67] as well as experiments, show that the splat morphology depends strongly on the particle size, velocity, and temperature upon impact. However, because droplets have large velocity, size, and surface temperature distributions when impacting on the substrate, the splat collection is tedious, and comprehensive studies are scarce and based on numerous assumptions. The acoustic emission used to monitor the impact of individual particles (see Ref 12) is also very difficult to interpret according to the same arguments presented for splat collection.

Much more precise information has been obtained due to the development of a two-color pyrometric technique to monitor the thermal evolution of individual droplets as they impact on a substrate.[54-56] Tests have been carried out with different kinds of sprayed materials (Nb or TiC) and different substrates (steel, glass, and alumina). In all cases, the thermograms show an almost instantaneous rise (much less than 1 msec) to the maximum temperature, followed by a gradual cooling for particles impacting in a completely molten state. A more gradual rise to the maximum temperature is observed if the particle has started to freeze before impact with an unveiled hotter internal liquid core. Such measurements also seem to show that the cooling rate is increased with the substrate temperature, which might be due to better flow of the molten particle on the hotter surface. Experiments related to the whole coating seem to confirm such results. The adhesion and cohesion of alumina coatings on cast iron substrates are increased by a factor of 4 when spraying on a substrate preheated to 400 °C, while maintaining the coating temperature of 400 °C during spraying and letting the coating and substrate cool slowly.[68] This shows the importance of a better understanding of the parameters controlling the flattening and solidification of droplets.

With a new technique using two pyrometers,[12,56] it is possible to determine the temperature particle prior to impact (2 mm ahead of the substrate), its velocity upon impact, its surface and temperature evolutions during impact, as well as its degree of flattening. For example, Fig. 14 illustrates the time-temperature evolution after impact for a 30-μm particle sprayed onto a steel substrate with an argon-hydrogen plasma jet. The measurement of the droplet surface temperature prior to impact confirms that the particle has started to cool (at about 60 mm downstream of the nozzle exit as shown by the statistical measurements in flight) and that the core is hotter than the surface. From this thermogram, the cooling rate of this particle during the first 10 μsec is estimated to be as high as 10^8 K/sec.

4.2 *Study of the Coating as a Whole during Spraying*

One of the key parameters to obtain high-quality coatings, as outlined in the introduction of this section, is to monitor the temperature of the coating during spraying. This can be achieved through a better knowledge of the heat flux distributions from the particles and the plasma jet. For particles, a few calorimeters have been developed.[67] For the plasma jet itself, assuming the heat flux is Gaussian allows one to determine its distribution (maximum flux and Gaussian radius).[69]

To monitor the surface temperature, thermocouples located in the substrate can only provide values related to the substrate, which may be widely different from the surface temperature (especially when spraying ceramics).[68] Infrared thermography permits one, with a previous calibration of the coating emissivity (which may vary in a wide range during spraying due for example to suboxides formation), to determine the surface temperature[70] of the coating.

However, the response time of the camera (about 0.1 sec) is too slow to follow the temperature variations of the passes (in the msec range), and infrared two-color pyrometry still needs to be developed to better understand the heat exchanges during spraying.

5. Conclusion

Although plasma spraying is probably one of the most versatile tools to apply a wide variety of coatings on almost any substrate, its development has been largely empirical over the last two decades. It is only during the past few years that new measurement techniques have been used to develop a better understanding of the complex phenomena involved and to improve process modeling.

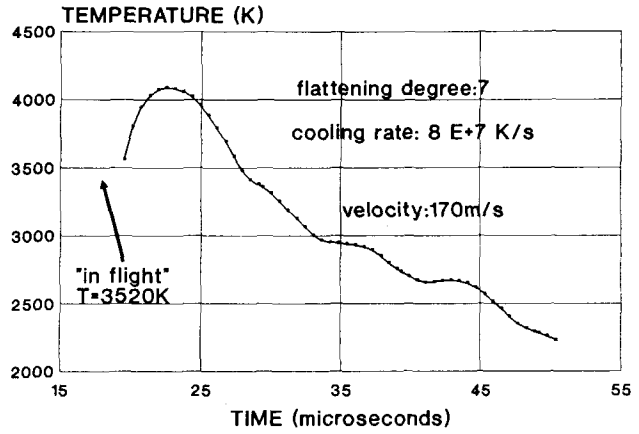

Figure 14 Time-temperature evolution after impact for a tungsten particle (–45 +22 μm) sprayed with an argon-hydrogen plasma jet (45 slm Ar, 15 slm H_2, I = 500 A, nozzle: 7-mm inner diameter, spraying distance 120 mm).

Computerized video-image processing has shown the important fluctuations undergone by the plasma jets and underlined the necessity to better understand the coupling between the arc root fluctuations and the cold gas flow in the plasma column fringes. Such measurements, however, imply the development of signal processing techniques to extract characteristic frequencies from noisy voltage, arc current, light intensity, and acoustic signals. These fluctuations induce a type of pulsed flow in the plasma jet, which contributes to the development of turbulence and pumping of the surrounding atmosphere. Pumped nitrogen concentration and temperature measurements by CARS, as well as LDA velocity measurements of small particles entrained and injected in the plasma gas, have shown that this pumping is of an engulfment type. Subsequently, the mixing of cold, dense air "bubbles" with the plasma is not as fast as was previously thought.

For the plasma jets, although computerized spectroscopic measurements are now well established, the meaning of the resulting temperatures has to be looked at very carefully due to the fluctuations, the surrounding atmosphere pumping, and the nonequilibrium effects. These effects are important, even at atmospheric pressure. However, such measurements permit comparison of the influence of the design and working parameters of plasma torches and optimization of them. A comparison of the spectroscopic temperatures with those deduced from enthalpy probes at distances greater than 30 mm from the nozzle exit shows a rather important discrepancy between these measurements. Enthalpy probes measure the temperature resulting from the plasma mixing with the surrounding atmosphere. Rayleigh scattering can be used to measure heavy species temperatures in regions where $T < 6000$ K, and this technique could be very useful for measuring heat transfer coefficients to a substrate in connection with heat flux measurements.

Enthalpy probes can also be used to determine the concentrations of plasma gas and surrounding atmosphere in the plasma jet as well as the jet velocities. For velocity measurements, the study of the light fluctuations, with a proper signal treatment, provides access to a simple determination of the axial plasma flow velocity.

For particles in flight, the statistical measurements of velocity, surface temperature, number density, and diameter of particles in flight have confirmed that they follow very different trajectories and undergo widely different heat treatments. However, one has to be aware that such measurements are not necessarily related to the same group of particles, even if the same measurement volume and time are considered, and their interpretation is not straightforward. Two-dimensional laser imaging confirms the trajectory dispersion induced by the same size and injection velocity distributions of the particles, as well as by the collisions of the particles with the injector wall resulting in non-negligible radial velocity distributions at the injector exit. This technique can be used to great advantage to optimize the powder injector location and injection angle. Particle vaporization, especially for particles in which the heat propagation is not negligible, is important. The spectroscopic measurements have shown, in regions where vapor clouds are symmetrical (where particle velocity is close to that of the plasma), the importance of their size (an order of magnitude greater than that of the particle). Such big vapor clouds modify the heat transfer between the plasma and the particle. However, techniques are still being developed to study these vapor clouds close to the substrate and to evaluate their importance for particle flattening. It should also be noted that the plasma jet length fluctuations, revealed by computerized video-image processing, raise the question of particle treatment: Should it be continuous, as commonly allowed, or are the particles heated more or less according to their time of passage in the fluctuating plasma jet?

Finally, the splats, collected at different distances and radii downstream of the nozzle exit, exhibit a wide variety of shapes and morphologies. Recently developed pyrometric techniques permit the measurement of particle velocity and temperature prior to impact, as well as the evolution of their temperature and surface (flattening degree) during flattening. They will probably contribute to a better understanding of how the splats are formed and the resulting contacts between the new in-coming splat and the previously deposited ones or the substrate. Such systematic measurements are of primary importance to control the thermomechanical properties of the coatings. However, such control also implies the development of new, fast (~10 kHz) infrared pyrometers to monitor the surface temperature of beads and passes during spraying.

References

1. N.N. Rykalin and V.V. Kudinov, *Pure Appl. Chem., 48*, 299 (1976).
2. J.H. Zaat, *Ann. Rev. Mater. Sci., 13*, 9 (1983).
3. *Thermal Spraying, Practice, Theory and Application*, American Welding Society, Miami (1985).
4. Technology Forecast, staff report *Advan. Mater. Proc., 133, 1*, 8 (1988).
5. P. Fauchais, A. Grimaud, A. Vardelle, and M. Vardelle, *Ann. Phys. Fr., 14*, 261 (1989).
6. J.F. Finke, R. Rodriguez, and C.G. Pentecost, in *Thermal Spray Research and Applications*, T.F. Bernecki, Ed., ASM International, Materials Park, 45 (1990).
7. R. Spores and E. Pfender, *Surf. Coat. Technol., 37*, 251 (1989).
8. P. Fauchais, J.F. Coudert, and M. Vardelle, in *Plasma Diagnostics*, Academic Press, New York, 349 (1989).

9. J. Dong and R.J. Kearney, "Plasma Gas Velocities in an Argon Jet at Atmospheric Pressure," *Plasma Chem. Plasma Proc.*, submitted for publication.
10. J.R. Finke and W.D. Swank, in *Thermal Spray Research and Applications*, T.F. Bernecki, Ed., ASM International, Materials Park, 39 (1990).
11. M.I. Boulos, *Proc. 2nd Plasma Technik Symposium, 1*, P. Huber and H. Eschnauer, Ed., Wolhen, Switzerland, 49 (1991).
12. A. Vardelle, M. Vardelle, and P. Fauchais, "Diagnostics for Particulate Vaporization and Interactions with Surfaces," *Pure Appl. Chem.*, accepted for publication.
13. F. Fauchais, J.F. Coudert, A. Vardelle, M. Vardelle, A. Grimaud, and P. Roumilhac, in *Advances in Coating Technology*, ASM International, Metals Park, 11 (1988).
14. J.F. Coudert, C. Delalondre, P. Roumilhac, O. Simonin, and P. Fauchais, "Modelling and Experimental Study of a Transferred Arc Stabilized with Argon in an Argon Atmosphere," *Plasma Chem. Plasma Proc.*, submitted for publication.
15. P. Roumilhac, Ph.D. thesis, University of Limoges, Mar (1990).
16. J.M. Leger, Ph.D. thesis, University of Limoges, Mar (1990).
17. E. Pfender, W.L.T. Chen, and R. Spores, in *Thermal Spray Research and Applications*, ASM International, Materials Park, 1 (1990).
18. B.A. Detering, J.R. Knibloc, and T.L. Eddy, in *Thermal Spray Research and Applications*, ASM International, Materials Park, 27 (1990).
19. J.R. Fincke, C.L. Jeffery, and S.B. Englert, *Mater. Res. Soc. Symp. Proc., 98*, 127 (1987).
20. T. Hoffman, *Advan. Mater. Proc., 140*(3), 37 (1991).
21. T.L. Eddy, J.D. Grandy, and B.A. Detering, "Heat Transfer in Thermal Plasma Processing," *HTD-161*, 57, 28th National Heat Transfer Conference, Minneapolis, Minnesota, K. Etemadi and J. Mostaghimi, Ed., (1991).
22. J.F. Coudert and P. Fauchais, "Plasma Flow Velocity Measurements in d.c. Arc Jets Using Cross Correlation Analysis of the Luminous Fluctuations," *Plasma Chem., Plasma Proc.*, submitted for publication.
23. J.R. Fincke, R. Rodriguez, and C.G. Pentecost, *Mater. Res. Soc. Symp. Proc., 190*, 207 (1991).
24. E. Pfender, J. Fincke, and R. Spores, *Plasma Chem. Plasma Proc., 1*, 529 (1991).
25. R. Spores and E. Pfender, *Surf. Coat. Technol., 37*, 251 (1989).
26. R. Spores, Ph.D. thesis, University of Minnesota, Minneapolis, Dec (1989).
27. S.C. Synder and J.D. Grandy, "Heat Transfer in Thermal Plasma Processing," *HTD-161*, 95, 28th National Heat Transfer Conference, Minneapolis, Minnesota, K. Etemadi and J. Mostaghimi, Ed., (1991).
28. J.F. Coudert and P. Fauchais, "The Influence of the Arc Fluctuations on the Temperature Measurements in D.C. Plasma Jets," TSM Annual Meeting (1992).
29. T.L. Eddy, J.M. Leger, J.F. Coudert, and P. Fauchais, "Heat Transfer in Thermal Plasma Processing," *HTD- 161*, 67, 28th National Heat Transfer Conference, Minneapolis, Minnesota, K. Etemadi and J. Mostaghimi, Ed., (1991).
30. T.L. Eddy, B.A. Detering, J.A. Batdorf, and P.G. Schenk, "Heat Transfer in Thermal Plasma Processing," *HTD-161*, 57 (1991).
31. P. Roumilhac, J.F. Coudert, and P. Fauchais, *Mater. Res. Soc. Symp. Proc., 190*, 227 (1991).
32. A.C. Eckbreth and T.J. Anderson, *Appl. Optics, 24*, 2731 (1985).
33. R.R. Autcliff and T.J. Anderson, *Appl. Optics, 24*, 2731 (1985).
34. R.J. Hall and A.C. Eckbreth, CARS: Application to Combustion Diagnostics, in *Laser Applications*, Vol. 5, J.F. Ready and R.K. Eaf, Ed., Academic Press, New York (1984).
35. A.J.D. Farmer and G.H. Haddad, *J. Phys. D Appl. Phys., 22*, 426 (1988).
36. Z. Wang and R.J. Kearney, *J. Quant. Spectrosc. Radiat. Transfer, 44*, 39 (1990).
37. J.R. Fincke and C.G. Pentecost, "Heat Transfer in Thermal Plasma Processing," *HTD, 161*, 101 (1991).
38. M. Brossa and E. Pfender, *Plasma Chem. Plasma Proc., 8*(1), 75 (1988).
39. Y.P. Chyou and E. Pfender, *Plasma Chem. Plasma Proc., 9*(2), 291 (1989).
40. M. Vardelle, A. Vardelle, P. Fauchais, and M. Boulos, *Am. Inst. of Chemical Engineers Journal, 29*, 236 (1981).
41. J. Lesinski, M. Mizera-Lesinska, J.C. Fanton, and M. Boulos, *Am Inst. of Chemical Engineers Journal, 27*, 252 (1981).
42. E. Pfender, *Pure Appl. Chem., 57*(9), 1179 (1985).
43. R. Spores and E. Pfender, in *Thermal Spray Technology, New Ideas and Processes*, ASM International, Materials Park, 85 (1989).
44. W.L. Bohm, M.U. Beth, and G. Nedda, *J.Q.S.R.T., 7*, 661 (1967).
45. A.W. Koch, K.D. Landes, G. Seeger, and W. Tiller, "Local Measurements of Gas Velocity in an Argon Plasma Jet," *Int. Inst. Welding*, Germany (1989).
46. A. Capetti and E. Pfender, *Plasma Chem. Plasma Proc., 9*(2), 329 (1989).
47. J.D. Grandy and R.J. Kearney, "Heat Transfer in Thermal Plasma Processing," *HTD, 161*, 107 (1991).
48. P. Fauchais, M. Vardelle, A. Vardelle, and J.F. Coudert, *Met. Trans., 20B*, 263 (1989).
49. J.A. Lewis and W.H. Gauvin, *AIChE, 19*, 982 (1973).
50. G. Frind, C.P. Goody, and L.E. Prescott, *6th International Symposium on Plasma Chemistry, 1*, 120 M.I. Boulos and R.J. Mury, Ed., Montreal, Quebec, Canada (1983).
51. W.C. Roman, W. Winter, A.A. Rotunno, K. Fessenden, and W. Willer, *Thermal Spray Research and Applications*, ASM International, Materials Park, 49 (1991).
52. T. Sakuta and M. Boulos, *9th International Symposium on Plasma Chemistry, 1*, 371 R. D'Agontino Ed., Pugnschiuso, Italy (1989).
53. M. Vardelle, state thesis, University of Limoges, July (1987).
54. C. Moreau, P.P. Cielo, M. Lamontagne, S. Dallaire, and M. Vardelle, *Meas. Sci. Technol., 1*, 807 (1990).
55. C. Moreau, P.P. Cielo, M. Lamontagne, S. Dallaire, J.C. Krapez, and M. Vardelle, *Thermal Spray Research and Applications*, ASM International, Materials Park, 19 (1991).
56. C. Moreau, M. Lamontagne, and P. P. Cielo, "Influence of the Coating Thickness on the Cooling Rates of Plasma Sprayed Particles Impinging on a Substrate," *Thermal Spray Research and Applications*, 3rd National Thermal Spray Conbference, Long Beach California, T.F. Bernecki Ed., ASM International. (1991).
57. A. Vardelle, J.M. Baronnet, M. Vardelle, and P. Fauchais, *Inst. Elec. Electron. Eng. Journal, PS8*, 417 (1980).
58. A. Vardelle, M. Vardelle, and P. Fauchais, *Plasma Chem. Plasma Proc., 2*, 255 (1982).
59. J. Mishin, M. Vardelle, J. Lesinski, and P. Fauchais, *J. Phys. E. Sci. Instr., 20*, 620 (1987).
60. M. Vardelle, A. Vardelle, P. Fauchais, and M. Boulos, *Am. Inst. of Chem. Engin. Journal, 34*(4), 567 (1988).
61. J.R. Fincke and C.L. Jeffery, *National Thermal Spray Conf. Proc.*, ASM International, Materials Park, 55 (1988).
62. G. Gouesbet, *Plasma Chem. Plasma Proc., 5*(2), 91 (1985).
63. M. Vardelle, A. Vardelle, C. Trassy, and P. Fauchais, *Plasma Chem. Plasma Proc., 11*(2), 185 (1991).
64. T.L. Eddy, B.A. Detering, and G.C. Wilson, in *Thermal Spray Research and Applications*, ASM International, Materials Park, 33 (1990).
65. J. Madjeski, *Int. J. Heat Mass Transfer, 19*, 1009 (1766).
66. R. McPherson, *J. Mater. Sci., 15*, 3141 (1980).
67. J.M. Houben, Ph.D. thesis, University of Eindhoven, Netherlands (1988)

68. L. Gyenis, A. Grimaud, O. Betoule, F. Monerie-Moulin, P. Fauchais, and M. Ducos, *2nd Plasma-Technik Symp.*, *1*, P.T. Wohlen, CH, 95 (1991).

69. F. Monerie-Moulin, F. Gitzhoffer, P. Fauchais, and M. Boulos, "Study of the Heat Flux Transmitted by a D.C. Ar-H_2 Plasma Spraying Jet to a Cold Substrate," TSM Annual Meeting, San Diego, Mar (1992).

70. L. Pawlowski, M. Vardelle, and P. Fauchais, *Thin Solid Films*, *94*, 307 (1982).